Calibrating an Optical Trap Using Polystyrene Beads

Emmy Blumenthal*
Boston University Department of Physics
CAS PY 571 — Introduction to Biophysics

Sam Fulton† and Catherine Miller‡
(Dated: March 19, 2023)

The calibration of optical traps is a critical step in the accurate measurement of forces and distances in experiments involving biological molecules and colloidal particles. In this report, we present a study on the calibration of optical trap tweezers using polystyrene beads. The linear relationship between the restoring force and displacement in the optical trap is established, and the primary calibration method involves the power spectral density of the time series. An alternative method using the auto-correlation function is also considered. We discuss the experimental setup, calibration procedures, sources of error, and limitations of the technique in detail. Our results provide estimates for the stiffness of the optical trap and the voltage-displacement response coefficient of the measuring apparatus.

All data, code, and figures are available at `https://github.com/emmyb-bu/PY571-Calibration-Lab`.

I. INTRODUCTION

Optical trap tweezers have become a widely used tool for studying the mechanical properties of biological molecules and colloidal particles. They offer a non-invasive method of manipulating small objects without the need for physical contact or labeling. Optical traps are created using focused laser beams that generate a gradient force capable of trapping and moving small particles.

Polystyrene beads are commonly used as model particles in the calibration of optical trap tweezers due to their well-defined size and optical properties. In this study, we use polystyrene beads to calibrate an optical trap. The primary calibration method utilized in this study involves the power spectral density of the time series, although an alternative method using the auto-correlation function is also considered. The experimental setup, calibration procedures, sources of error, and limitations of the technique are discussed in detail.

In an optical trap, the restoring force is directly proportional to the displacement of the trapped particle, but this relationship only holds when the displacement is small. In experiments, the displacement is typically small, resulting in a linear relationship between the restoring force and the displacement. This linear relationship is essential for determining the stiffness of the optical trap and the mechanical properties of the trapped particle.

The results obtained in this study provide estimates for the stiffness of the optical trap and the voltage-displacement response coefficient of the apparatus that measures the displacement of the polystyrene bead in the trap. These estimates are essential for accurate measurements of forces and distances in subsequent experiments. The limitations and implications of the results will be further discussed in subsequent sections.

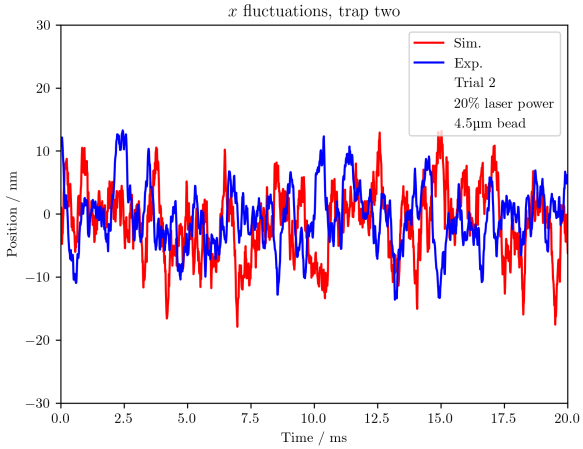

FIG. 1. Comparison of a measured time series and simulated Langevin dynamics with corresponding fitted parameters. The time series are distinct from each other because of the nature of the statistical system. However, we observe that the magnitude, profile, and time-scale of fluctuations in both curves are very similar, supporting qualitatively that the observed data follows Langevin dynamics.

II. METHODS

A. Trap properties

The Lumicks optical tweezer we used has two traps and an apparatus to measure displacement of a bead in

* emmyb320@bu.edu
† sjfulton@bu.edu
‡ cmiller6@bu.edu

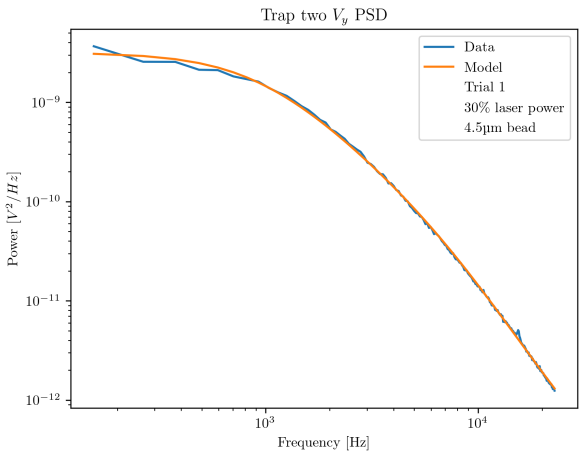

FIG. 2. Fitting the Langevin model power spectrum to some collected data. The strong agreement between the curves indicates supports the hypothesis that the observed data is produced by Langevin dynamics.

a vertical and horizontal direction in each trap. The reported signal is in voltage, so it is necessary to find a conversion factor, β, from voltage to displacement:

$$x = \beta V. \tag{1}$$

For small displacements, the restoring force on the optical tweezer is linear with stiffness κ,

$$F = -\kappa x. \tag{2}$$

Our objective is to estimate the values of β and κ. To do this, we will use two methods: fitting to the power spectral density and signal autocorrelation; this constitutes calibration of the optical trap. We perform this analysis in each direction, for each trap, and for beads of sizes 2.14 µm, 4.5 µm. For the 2.14 µm beads, we tested the trap at 10%, 15%, and 20% laser power. For the 4.5 µm beads, we tested the trap at 10%, 20%, and 30% laser power.

B. Power spectral density of Langevin dynamics

We assume the beads undergo Langevin dynamics, governed by the stochastic differential equation,

$$\ddot{x} = -\kappa x - \gamma m \dot{x} + \sqrt{2m\gamma k_B T} R(t), \tag{3}$$

where $\gamma = 6\pi\eta r$ is the drag coefficient, η is the viscosity of the fluid in which the dynamics take place, r is the radius of the bead, m is the mass of the bead, and $R(t)$ are random kicks modeled as a Gaussian stochastic process with $\langle R(t)\rangle = 0$ and $\langle R(t)R(t')\rangle = \delta(t-t')$. In the viscous, Markovian limit, the power spectral density of x is,

$$P_x(f) = \langle|\tilde{x}(f)|^2\rangle = \frac{1}{2\pi^2}\frac{D_{\text{phys}}}{f_c^2 + f^2}, \tag{4}$$

where $D_{\text{phys}} = k_B T/\gamma$ is the diffusion constant and $f_c = \kappa/(2\pi\gamma)$ is the so-called 'corner frequency.'

Given the measured voltage signal $V(t)$, we can its power spectral density to the model,

$$P_V(f) = \langle|\tilde{x}^2(f)|^2/\beta^2\rangle = \frac{1}{2\pi^2}\frac{D_{\text{meas}}}{f_c^2 + f^2}, \tag{5}$$

where f_c and $D_{\text{meas}} = D_{\text{phys}}/\beta^2$ are fit parameters; note that D_{meas} has dimensions of [voltage]^2/[time]. Therefore, if we have the fit parameters, we can estimate,

$$\beta = \sqrt{\frac{D_{\text{phys}}}{D_{\text{meas}}}}, \qquad \kappa = 2\pi\gamma f_c. \tag{6}$$

The fitting software used reports estimates for errors in fitted parameters. We can use the error estimates δD_{meas} and δf_c to find error estimates for the calibrated quantities,

$$\delta\beta = \left|\frac{\partial\beta}{\partial D_{\text{meas}}}\right|\delta D_{\text{meas}} = \frac{1}{2}\sqrt{\frac{D_{\text{phys}}}{D_{\text{meas}}^3}}\delta D_{\text{meas}}, \tag{7}$$

$$\delta\kappa = \left|\frac{\partial\kappa}{\partial f_c}\right|\delta f_c = 2\pi\gamma\delta f_c. \tag{8}$$

See figure 2 for an example of the measured power spectrum and the fitted model.

C. Autocorrelation functions

Given the position time series of Langevin dynamics, the autocorrelation function is given by,

$$C_x(t) = \langle x(t'+t)x(t')\rangle_{t'} = \frac{k_B T}{\kappa}e^{-t/\tau}, \tag{9}$$

where, $\tau = \gamma/\kappa$. Using $x(t) = V(t)/\beta$, we can find,

$$C_V(t) = \langle V(t'+t)V(t')\rangle_{t'} = \frac{C_x(t)}{\beta^2}. \tag{10}$$

If we then fit $\log[C_V(t)/V_0^2]$, where V_0 is some voltage scale, to the linear model $a + bx$, we have,

$$\kappa = -\gamma b, \qquad \beta = \sqrt{\frac{k_B T}{-\gamma b V_0^2}e^{-a}}. \tag{11}$$

III. RESULTS

We successfully collected data for the bead sizes 2.14 µm, 4.5 µm in the x and y directions and in the two traps. For each of these cases, we performed two measurements. Time series data of the voltage for each sample was recorded for approximately 15 s.

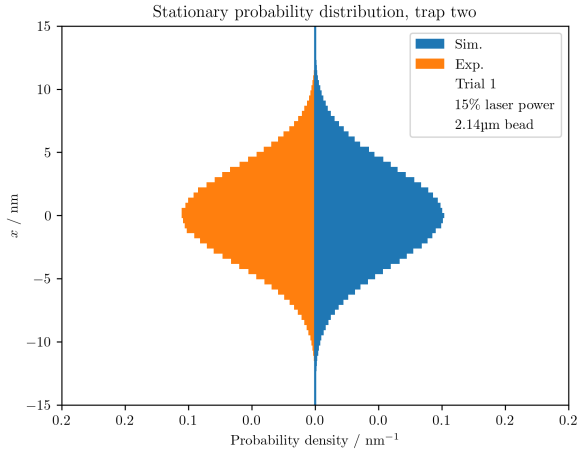

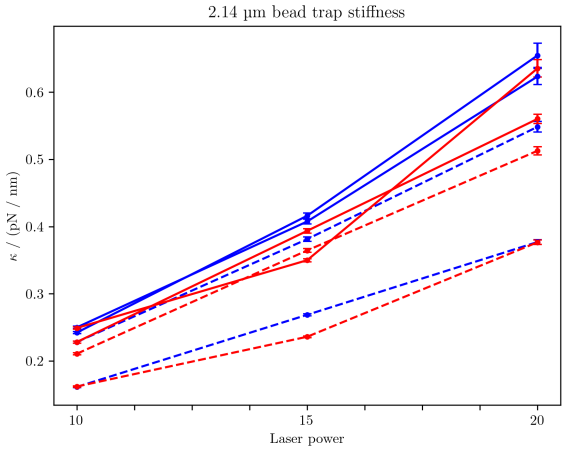

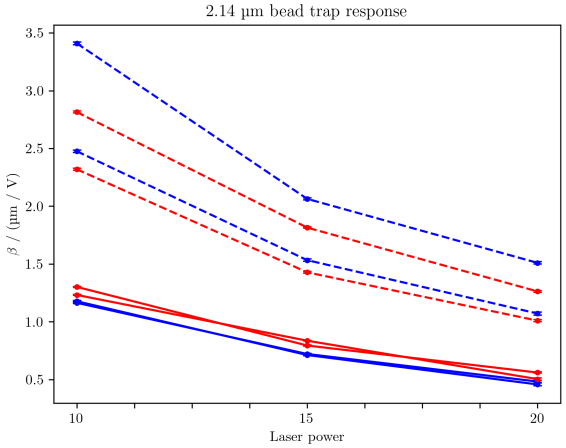

FIG. 3. Time-averaged stationary distribution for collected time series (left) and simulated Langevin dynamics with corresponding fitted parameters (right). The form and width of the distributions seem to agree, supporting the hypothesis that the collected data is due to Langevin dynamics.

FIG. 4. For the 2.14 μm diameter bead, top: trap stiffness with varying laser power; bottom: voltage-displacement response coefficient with varying laser power. Solid lines represent data collected from trap one; dashed lines represent data collected from trap two. Blue lines represent data computed when measuring in the x-direction; red lines represent data computed when measuring in the y-direction. Note that there are two lines for each combination of these styles, representing that we performed two trials for each of these cases. The calculation of error bars is given in lines 7 and 8. For 4.5 μm diameter beads, see figure 5.

A. Power spectral density method

We use the Pylake software package to produce and fit the power spectral density; see figure 2 for an example of this fit. For the fit parameters, we assumed values of the drag coefficient and viscosity of water for an ambient temperature of 25 °C. Additionally, we took the density of polystyrene to be $1.047 \times 10^3\,\mathrm{kg\,m^{-3}}$. After fitting data to the model in line 5 and using the relations in line 6, we obtain fitted parameters and perform simulations of Langevin dynamics using the BAOAB integrator with the fitted parameters. This allows us to compare the dynamics observed in the optical trap to the Langevin model; we compare the data by juxtaposing time series (figure 1) to see the time-scale of fluctuations and by comparing time-averaged stationary probability distributions (figure 3). In order to produce compelling simulation data, we had to choose the step save rate of the simulation integrator to match the sampling rate of the experimental data. When this adjustment is not made, rare, quick-lived fluctuations that are underrepresented in the experimental data will be represented properly in the simulation data. This can be seen by observing that the time scale $m/\gamma \sim 10^{-6}\,\mathrm{s}$ is an order of magnitude smaller than the sampling rate, $1.28 \times 10^{-5}\,\mathrm{s}$, of the optical trap detector.

After fitting data for each simulation, we assemble our analyzed data and plot the responses and stiffnesses for different values of laser power. See figures 4 and 5.

Additionally, we expect the standard deviation, σ_x, of the time-averaged stationary distribution of Langevin dynamics to satisfy,

$$\left\langle \frac{1}{2}\kappa x^2 \right\rangle = \frac{k_B T}{2} \implies \sigma_x = \sqrt{\frac{k_B T}{\kappa}}, \tag{12}$$

due to the equipartition theorem. For each of the time series collected, we plot the measured standard deviations of the time-averaged stationary distributions along with the value of the standard deviation predicted by the equipartition theorem. For the various laser powers, the predicted and measured standard deviations are plotted in figures 6 and 11.

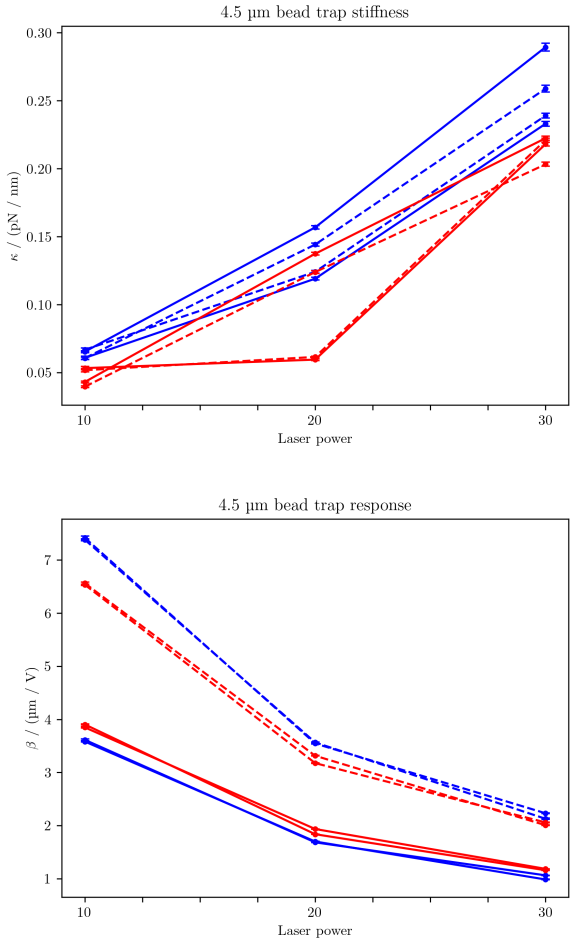

FIG. 5. The same results as displayed in figure 5 are shown here but with the 4.5 µm diameter bead. There appears to be some outlying data for the stiffness at 20% laser power in the y-direction in both the first and second trap.

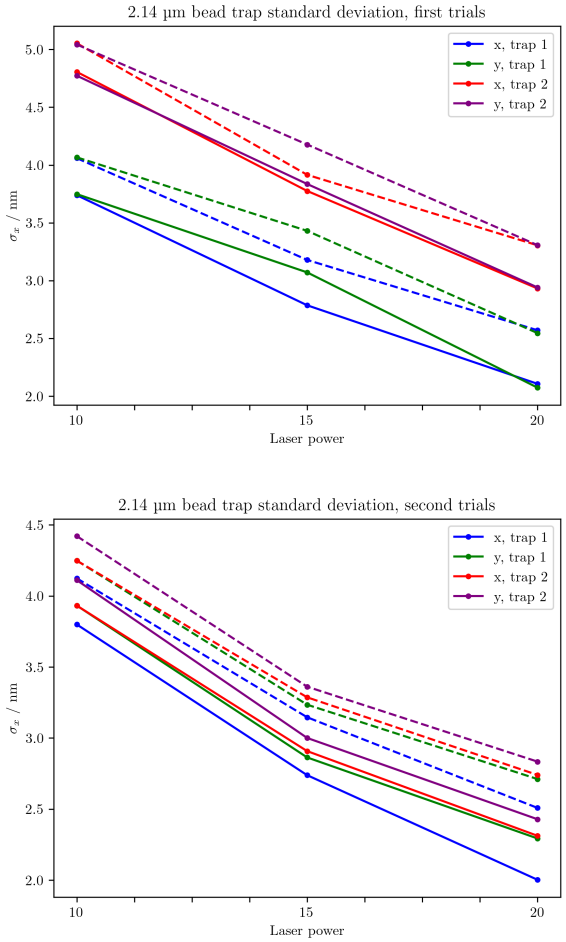

FIG. 6. Comparison of standard deviations of the time-averaged stationary distribution as measured from the time series (solid lines) and predicted by the equipartition theorem (dashed lines) for the 2.14 µm diameter bead.

B. Autocorrelation functions

The autocorrelation functions for the presented data seems to follow the exponential model presented in equation 9 very well. See figure 7 for an example of this data and the associated fit. In general, the stiffness and response coefficient values calculated from the autocorrelation function method match the values calculated from the power spectral density method with a relative error of 0.5% to 10%. A file contained associated data and fitted parameters is included with this manuscript.

IV. DISCUSSION

Before discussing the results and limitations of the calibration presented here, we first turn to understand one aspect of Langevin dynamics.

A. Effect of viscosity on Langevin dynamics

In figures 8, 9, 10 we show the results of simulating Langevin dynamics for many values viscosity values, all multiples of the viscosity of water. The simulations were performed with $\eta_{\text{water}} = 0.89\,\text{cP}$, $m = 50\,\text{pg}$, $\gamma = 37.7\,\text{pg}\,\mu\text{s}^{-1}$, $k_BT = 4.185\,\text{pN}\,\text{nm}$, time step $1\,\mu\text{s}$, and total simulation time $10\,\text{s}$; these parameters correspond to a $4.5\,\mu\text{m}$ diameter bead. We see in figure 8 that the time scale of fluctuations changes with increasing viscosity, but the absolute magnitude of fluctuations does not seem to vary. This is also apparent in figure 10, where we see that the slope of autocorrelation function on the log-linear plot decreases with increasing η, reflecting how the time scale of fluctuations is directly proportional to the viscosity. In figure 9, we see that the time-averaged stationary distribution of the simulated Langevin dynamics does not depend on viscosity. It is not difficult to show, by averaging a test function,

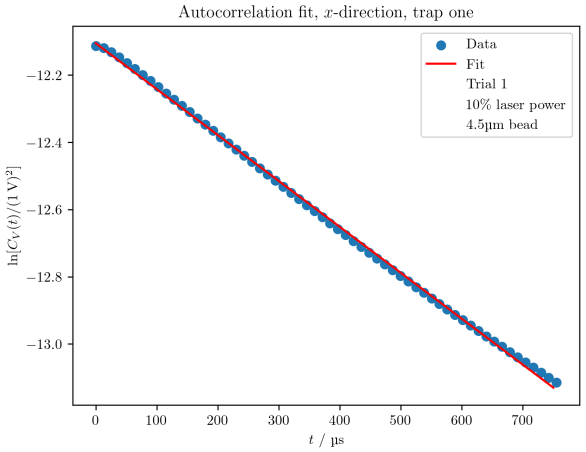

FIG. 7. Autocorrelation function of measured voltage time series. The above exponential fit seems to be quite good, indicating that the observed time series likely represents Langevin dynamics.

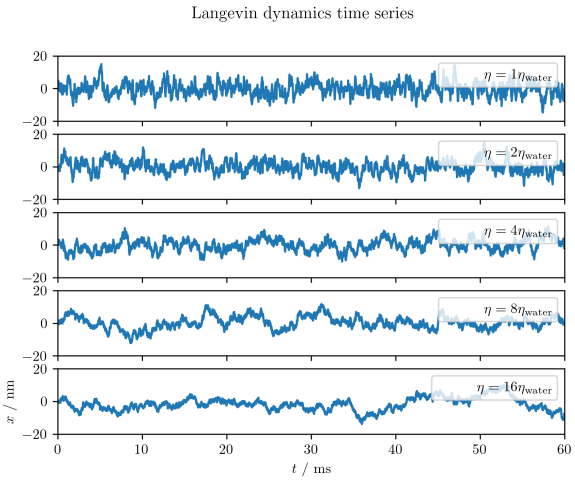

FIG. 8. Time series data of simulations of Langevin dynamics for various viscosities. As the viscosity is increased, the time scale of fluctuations increases proportionally, but the absolute magnitude of the fluctuations remains unchanged. See section IV A for simulation parameters.

that the stationary distribution of Langevin dynamics is the Boltzmann distribution. The Boltzmann distribution describes the probability of occupying a certain state in terms of the energy of the state, not in terms of dynamic properties; therefore, we expect that viscosity should have no effect on the time-averaged distribution.

B. Discussion of calibration procedure

By modeling the recorded data as Langevin dynamics, we were able to extract stiffnesses and response coefficients. We see in both figures 4 and 5 that as the laser power is increased, the stiffness increases, as expected. Additionally, the response coefficients decrease with increasing laser power, likely due to optical effects. In figures 6 and 11, when we compare the measured standard deviation of the stationary probability distribution to the value predicted by the equipartition theorem, we see that the measured value is consistently less. This is likely due to the time-scale at which the dynamics are sampled by the measurement apparatus. By the Onsager regression

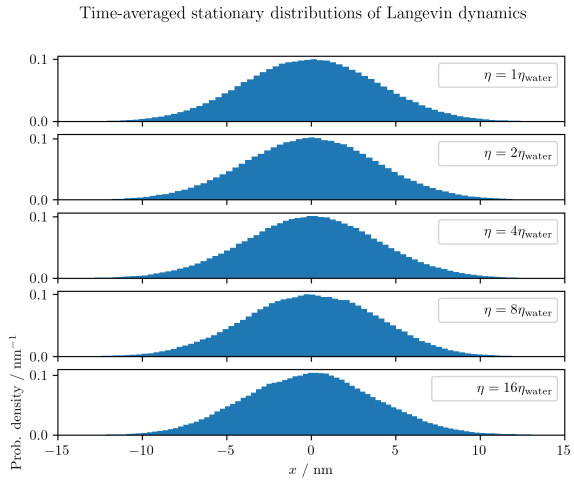

FIG. 9. Time-averaged histograms for stationary distributions of Langevin dynamics simulated with various values of viscosity, η. The stationary distribution is independent of the drag coefficient, γ, that depends on the viscosity. When time-averaging Langevin dynamics for long duration, one can show that the stationary distribution obeys Boltzmann statistics, which only depend on energy of a realized microstate.

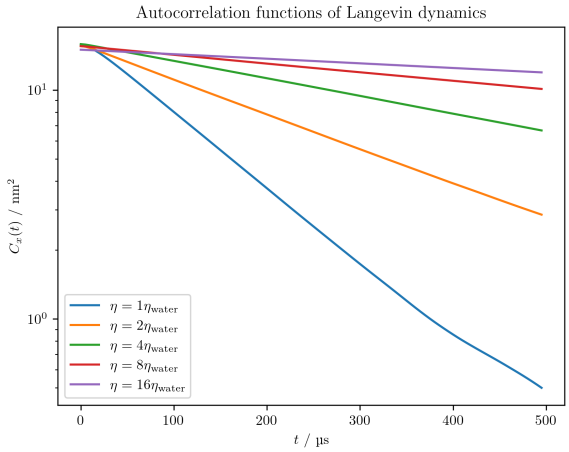

FIG. 10. Autocorrelation functions of simulated Langevin dynamics data for various values of viscosity, η. The exponential decay of the autocorrelation of Langevin dynamics is given in equation 9 and has a rate $1/\tau \propto 1/\eta$; therefore, we expect the slope of the autocorrelation functions on a log-linear plot to be inversely proportional to the viscosity.

hypothesis and the fluctuation-dissipation theorem, the time scale of the duration of rare fluctuations scale with $\gamma/m \sim 1 \times 10^{-6}$ s which is an order of magnitude smaller than the sampling rate of the apparatus. Therefore, in the collected data, the tails of the actual stationary distribution are under-sampled, leading to a systematic bias towards a smaller standard deviation than expected given an apparatus with an arbitrarily fast sampling rate.

Finally, it seems that fitting the autocorrelation function was a successful method, but the nature of a finite sample time limits the amount of data that can be used in a fit, especially in cases where $\tau = \gamma/\kappa \sim$ (bead diameter)/(laser power) is very short. This is because the data-estimated autocorrelation function $C_x(t)$ can only decay so much before it hits a plateau which appears only because the expected value is computed by averaging over a finite amount of data, leading to fluctuations about the actual expected value. This plateau in the autocorrelation function is a result of practical numerical and data limitations, not any underlying physical principle. Therefore, calibrating parameters with the autocorrelation function was successful for some collected data but less so for others. However, creating and visualizing the exponential fits as in figure 7 further supports that we are working with Langevin dynamics in this trap.

All data and code used in analysis for this report can be found in the repository at `https://github.com/emmyb-bu/PY571-Calibration-Lab`.

V. CONCLUSION AND ACKNOWLEDGMENTS

Through various methods, we were able to successfully demonstrate that the motion inside the optical trap on the time, length, and energy scales considered constitutes Langevin dynamics. We successfully explored two methods to calibrate the optical trap and have a deeper understanding of the methods used in the automatic calibrator in the Lumicks software and the physics of the trap itself.

EB thanks their group members CM and SF. Members of our lab group thank Masha Kamenetska, Brian Dawes, and Favian Liu for their support, guidance, and direction in this lab project. We additionally thank Dr. Kamenetska's research group for providing their Lumicks optical trap tweezer for educational purposes. The inspiration, methods, and many formulas were taken directly from the provided paper by Volpe, et. al.

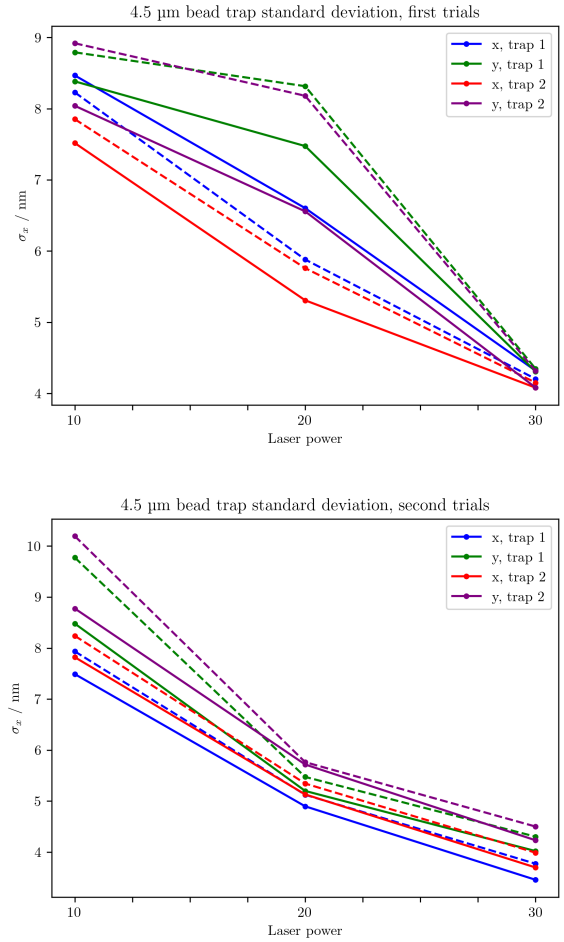

FIG. 11. Just as in figure 6, comparison of standard deviations of the time-averaged stationary distribution as measured from the time series (solid lines) and predicted by the equipartition theorem (dashed lines) but for the 4.5 µm diameter bead.